ELSEVIER

Polymer 42 (2001) 5463–5469

polymer

www.elsevier.nl/locate/polymer

Miscibility and interactions in blends of carboxyl-containing polysiloxane with poly(1-vinylimidazole)

X. Li[a], S.H. Goh[a,*], Y.H. Lai[a], A.T.S. Wee[b]

[a]*Department of Chemistry, National University of Singapore, 3 Science Drive 3, Singapore, Singapore 117543*
[b]*Department of Physics, National University of Singapore, 3 Science Drive 3, Singapore, Singapore 117543*

Received 28 March 2000; received in revised form 18 September 2000; accepted 12 December 2000

Abstract

The miscibility of poly(3-carboxypropylmethylsiloxane) (PSI100) and poly(3-carboxypropylmethylsiloxane-*co*-dimethylsiloxane) (PSI*X*, $X = 76, 60, 41, 23$ or 9, denoting the mole percentage of 3-carboxypropylmethylsiloxane unit in the copolymer) with poly(1-vinylimidazole) (PVI) was studied. PSI9 is miscible with PVI when the blend contains 80 wt% PVI. However, the other PSI*X* samples are miscible with PVI over the entire composition range. Most of the miscible PSI*X*/PVI blends show positive deviations in their glass transition temperature values. None of the miscible blends shows a lower critical solution temperature behavior prior to degradation. Fourier transform infrared spectroscopy and X-ray photoelectron spectroscopy show that some of the imidazole nitrogens are protonated by the carboxylic acid groups, leading to ionic interactions.

Keywords: Miscibility; Carboxyl-containing polysiloxane; Poly(1-vinylimidazole)

1. Introduction

It is well recognized that the formation of a miscible blend generally arises from a favorable intermolecular interaction between the two component polymers. Therefore, the introduction of small amounts of complementary functional groups into the polymers will promote the formation of miscible blends [1–13]. For example, Katime et al. [13] recently reported that while poly(*N*,*N*-dimethylacrylamide) (PDMA) is immiscible with poly(vinyl acetate), it is miscible with poly(vinyl acetate-*co*-vinyl alcohol) containing 56 mol% or more of vinyl alcohol units. Miscibility arises from hydrogen-bonding interactions between the hydroxyl groups in the vinyl alcohol units and the carbonyl groups in PDMA.

Because of the lack of interacting groups, poly(dimethylsiloxane) (PDMS) is generally immiscible with other polymers. Interacting groups have been incorporated into PDMS to promote miscibility [14,15]. We have recently reported that poly(3-carboxypropylmethylsiloxane-*co*-dimethylsiloxane) containing 23 mol% or more carboxylic acid group is miscible with poly(4-vinylpyridine) (P4VPy) and poly(2-vinylpyridine) (P2VPy) [16]. Fourier transform infrared spectroscopy (FT-IR) and X-ray photoelectron spectroscopy (XPS) show the existence of hydrogen-bonding interactions between the carboxylic acid groups and the pyridine nitrogens.

In view of the higher basicity of imidazole ($pK_b = 7.05$) than that of pyridine ($pK_b = 8.75$), we have studied the miscibility of poly(1-vinylimidazole) (PVI) with several proton-donating polymers [17,18]. Depending on their acidity, the proton-donating polymers interact with PVI through hydrogen-bonding or ionic interactions. In this paper, we report the miscibility of poly(3-carboxypropylmethylsiloxane) (PSI100) and poly(3-carboxypropylmethylsiloxane-*co*-dimethylsiloxane) (PSI*X*, $X = 76, 60, 41, 23$ or 9, denoting the mole percentage of 3-carboxypropylmethylsiloxane unit in the copolymer) with PVI. It is envisaged that PSI*X* will interact more strongly with PVI than with P4VPy or P2VPy.

2. Experimental

2.1. Materials

1-Vinylimidazole (Fluka Chemika-Biochemika Company) was distilled at 78–79°C/13 mmHg. PVI was prepared by solution polymerization using 2,2′-azobis(isobutyronitrile) (AIBN) as initiator. 1-Vinylimidazole (20 ml) was dissolved in 50 ml absolute ethanol and dry nitrogen was bubbled through the solution with vigorous stirring. AIBN (0.04 g)

* Corresponding author. Tel.: +65-874-2844; fax: +65-779-1691.
E-mail address: chmgohsh@nus.edu.sg (S.H. Goh).

0032-3861/01/$ - see front matter
PII: S0032-3861(01)00015-5

Table 1
Characteristics of polymers

	PSI9	PSI23	PSI41	PSI60	PSI76	PSI100
T_g (°C)	−104	−85	−55	−41	−29	−9
M_n (kg mol^{-1})	25	26	30	23	14	6.6
M_w/M_n	2.3	2.2	2.2	2.2	2.0	1.6

was added to the solution and polymerization was carried out at 70°C for 40 h. PVI was obtained by precipitating the ethanol solution in excess THF/hexane (3:8, v/v) solution. The polymer was washed repeatedly with the non-solvent mixture and dried in vacuo at 80°C. The weight-average molecular weight (M_w) and the number-average molecular weight (M_n) are 89 and 60 kg mol^{-1}, respectively. The glass transition temperature (T_g) is 163°C.

The synthesis and characterization of PSI*X* were reported previously [16]. The main characteristics of PSI*X* are summarized in Table 1.

2.2. Preparation of blends

Polymer blends with varying compositions were obtained by mixing appropriate amounts of ethanol/water (1:1) solutions (1% w/v) of PSI*X* and PVI. Initial removal of the solvent was done on a hot plate at 70°C. The blends were then dried in a vacuum oven at 80°C for 2 weeks. The dried blends were ground to fine powder and stored in a desiccator.

2.3. T_g measurements

The glass transition temperatures (T_gs) of various samples were measured with a TA Instruments 2920 differential scanning calorimeter using a heating rate of 20°C min^{-1}. Each sample was subjected to several heating/cooling cycles to obtain reproducible T_g values. The initial onset of the change of slope in the DSC curve is taken to be the T_g.

2.4. LCST behavior

All the miscible blends were examined for the existence of lower critical solution temperature (LCST) behavior. A film was sandwiched between two microscope coverglasses and heated in a Fisher–Johns melting-point apparatus at a heating rate of about 10°C min^{-1}. The optical appearance of the film was observed with a magnifying glass attached to the apparatus. A transparent film that turns cloudy upon heating indicates the existence of a LCST behavior.

2.5. FT-IR characterization

FT-IR spectra were recorded on a Bio-Rad 165 FT-IR spectrophotometer; 64 scans were signal-averaged with a resolution of 2 cm^{-1}. Samples were prepared by dispersing the blends in KBr and compressing the mixtures to form disks. Spectra were recorded at 130°C to exclude moisture, using a SPECAC high-temperature cell equipped with an automatic temperature controller, which was mounted in the spectrophotometer.

2.6. XPS measurements

XPS measurements were carried out on a VG Scientific ESCALAB spectrometer using a MgKα X-ray source (1253.6 eV photons). Various blends were ground to fine powders and were then mounted on a standard sample stud by means of a double-sided adhesive tape. The X-ray source was run at 12 kV and 10 mA. To compensate for surface charge effects, all core-level spectra were referenced to the C1s neutral carbon peak at a binding energy (BE) of 285.0 eV. The pressure in the analysis chamber was maintained at 10^{-8} mbar or lower during measurements. All spectra were obtained at a take off angle of 75° and were curve-fitted with VGX-900I software. In spectral deconvolution, the widths (fwhm) of Gaussian peaks were maintained constant for all components in a particular spectrum.

3. Results and discussion

3.1. Miscibility of blends

PDMS is immiscible with PVI throughout the entire composition range as shown by the opacity of the blends and the existence of two T_gs corresponding to those of the component polymers.

A PSI9/PVI blend containing 80 wt% PVI was transparent, and it showed one T_g, indicating that the blend is miscible. In contrast, the other PSI9/PVI blends were opaque and each showed two T_gs, indicating immiscibility. As shown in the Fig. 1, the lower T_g values of the immiscible blends are close to that of PSI9 and the upper T_g values are substantially lower than that of PVI, indicating the presence of PSI9 in the PVI-rich phase. In comparison, all the PSI9/P4VPy and PSI9/P2VPy blends are immiscible [16].

All the PSI23/PVI blends were transparent and each

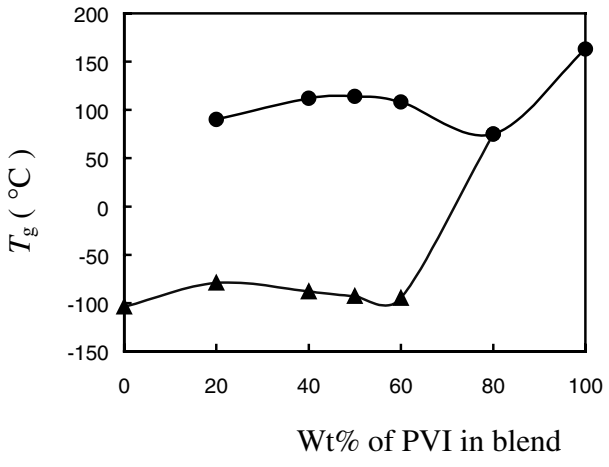

Fig. 1. T_g-composition curve of PSI9/PVI blends.

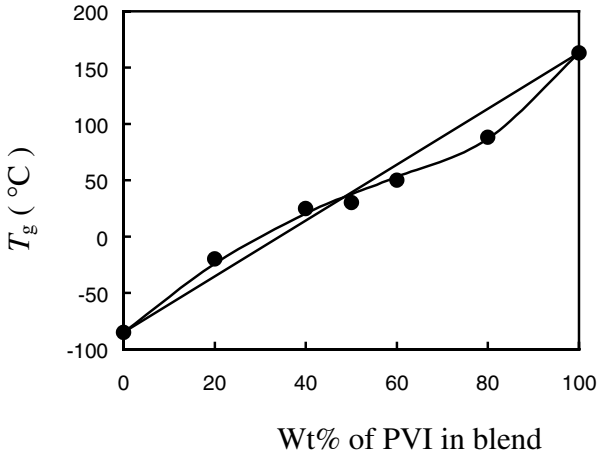

Fig. 2. T_g-composition curve of PSI23/PVI blends ($k = 3.6$, $q = 21$).

blend showed the existence of a single T_g. The T_g-composition curve of the PSI23/PVI blends is S-shaped (Fig. 2). On the other hand, the T_g-composition curves of miscible PSI23/P4VPy and PSI23/P2VPy blends are concave [16]. The results show that PSI23 is miscible with PVI. Therefore, the presence of 23 mol% carboxypropyl group in PSI*X* is sufficient to achieve miscibility with PVI throughout the entire composition range.

Similarly, PSI41, PSI60, PSI76 and PSI100 are all miscible with PVI as shown by the transparency of the blends and the existence of a single T_g in each blend. Figs. 3 and 4 show the T_g-composition curves of two of the miscible blend systems. When the carboxypropyl content in the PSI*X* is above 41 mol%, the T_g value of each blend is higher than that calculated from the linear additivity rule, leading to a convex curve. All the T_g-composition curves can be fitted by the Kwei equation [19,20]

$$T_g(\text{blend}) = [(w_1T_{g1} + kw_2T_{g2})/(w_1 + kw_2)] + qw_1w_2$$

where w_i and T_{gi} are the weight fraction and T_g of polymer i in the blend, respectively, and k and q are fitting constants.

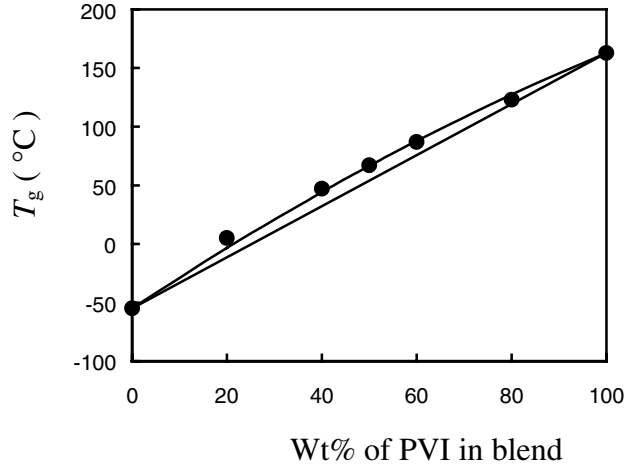

Fig. 3. T_g-composition curve of PSI41/PVI blends ($k = 1$, $q = 50$).

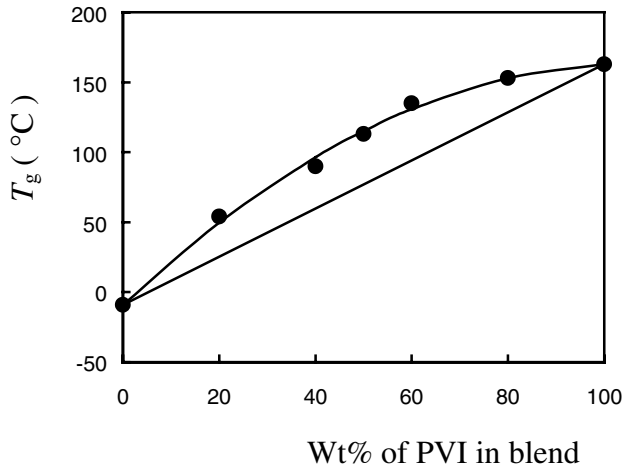

Fig. 4. T_g-composition curve of PSI100/PVI blends ($k = 1$, $q = 152$).

As shown in the figures, the T_g-composition curve can be fitted by the Kwei equation with $k = 3.6$, $q = 21$ for PSI23/PVI blends, and $k = 1$ and q values of 152, 128, 83 and 50 for PSI100/PVI, PSI76/PVI, PSI60/PVI and PSI41/PVI, respectively. Kwei [19] pointed out the term $(w_1T_{g1} + kw_2T_{g2})/(w_1 + kw_2)$ in the equation is a commonly used expression for the T_g of polymer mixtures which can be derived formally by using the additive rule of the entropy or the volume of the mixture, and the quadratic term qw_1w_2 is proportional to the number of specific interactions in the blends. The mixing term is concave toward the weight-average line where the interaction term is convex toward it. The combination of these two terms may result in the S-shaped curve as shown in Fig. 2. When the interaction term predominates (larger q value), the T_g-composition curve will then be convex as shown in Figs. 3 and 4. The q value increases with increasing carboxypropyl content of PSI*X*, reflecting an increase in the number of interactions. In this respect, there are a larger number of interactions in the PSI100/PVI blends than in poly(*p*-vinylphenol)/PVI blends ($q = 107$) and in poly(2-hydroxypropyl methacrylate)/PVI blends ($q = 90$) [17]. The changes in the shape of T_g-composition curves, from S-shaped curve to convex curve, and the q value with copolymer composition are in fact the result of increasing number of carboxypropyl groups.

The q values of the PSI*X*/PVPy blends are lower than those of the corresponding PSI*X*/PVI blends, indicating that the interactions in the PSI*X*/PVPy blends are weaker than those in the PSI*X*/PVI blends. Furthermore, only the T_g-composition curves of PSI100/P4VPy and PSI100/P2VPy blends are convex whereas the other curves are S-shaped [16].

The miscible PSI23/P4VPy and PSI23/P2VPy blends developed cloudiness upon heating to 170–200°C, showing the existence of LCST behavior [16]. However, all the miscible PSIX/PVI blends degraded before phase separation could be induced by heating. The absence of LCST behavior

of PSI23/PVI blends may be taken to indicate that PVI interacts more strongly with PSI23 than P4VPy and P2VPy do.

Therefore, the LCST behavior of the blends and the shapes of the T_g-composition curves suggest that the interactions between PVI and PSI*X* are stronger than those between PVPy and PSI*X*. It will be shown in the following sections that PVI interacts with PSI*X* through ionic interactions instead of hydrogen-bonding interactions.

3.2. FT-IR Characterization

Various PSI100/PVI blends were studied by FT-IR at 130°C, focusing on the hydroxyl stretching region and carbonyl stretching region of PSI100, and on the ring-stretching modes of imidazole in the blends. The spectra of the component polymers and all the blends in these regions are shown in Figs. 5–7.

Fig. 5 shows the spectra in the hydroxyl region of PSI100/PVI blends, along with those of the pure components. PSI100 exhibits a broad band around 3100 cm^{-1} and a satellite band around 2620 cm^{-1}, which can be attributed to dimeric carboxylic acid groups as commonly observed in other carboxylic acids [21–23]. Upon mixing PSI100 with PVI, the hydroxyl stretching region shows an increasing contribution at wavenumbers higher than those corresponding to the dimers. As the PVI content in the blend increases, this change becomes more distinct. Apparently, the dimeric association of carboxylic acid groups is replaced by interpolymer interactions. Fig. 5 also shows a remarkable shift of the satellite band (2620 cm^{-1}) towards a lower wavenumber and its intensity increases with increasing PVI content in the blends. Lippert et al. [24] have reported the FT-IR spectra of protonated PVI. They found the N–H stretching vibrations (in $PVIH^+$) at 2480 and 2610 cm^{-1}. With the formation of $PVIH^+$, the satellite band of the dimeric carboxylic acid groups around 2620 cm^{-1} disappears and the N–H stretching vibration at 2480 and 2610 cm^{-1} appeared gradually. As a result, the satellite band shifts towards a lower wavenumber.

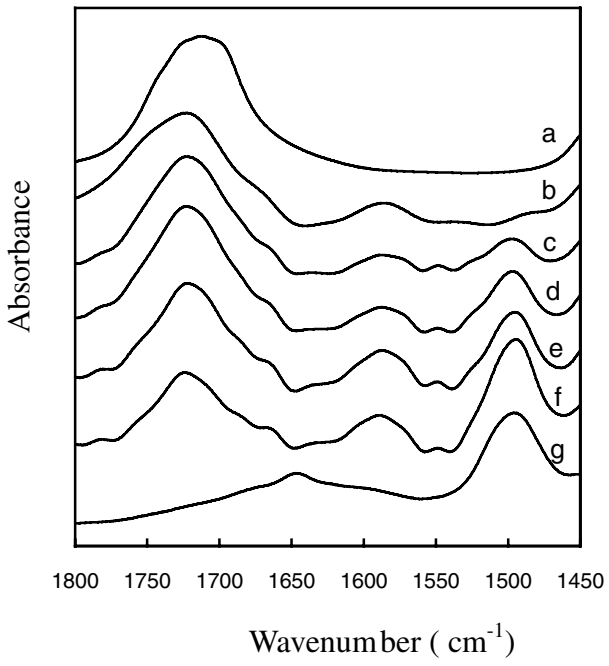

Fig. 6. FT-IR spectra of PSI100/PVI blends: (a) 0; (b) 20; (c) 40; (d) 50; (e) 60; (f) 80 and (g) 100 wt% PVI.

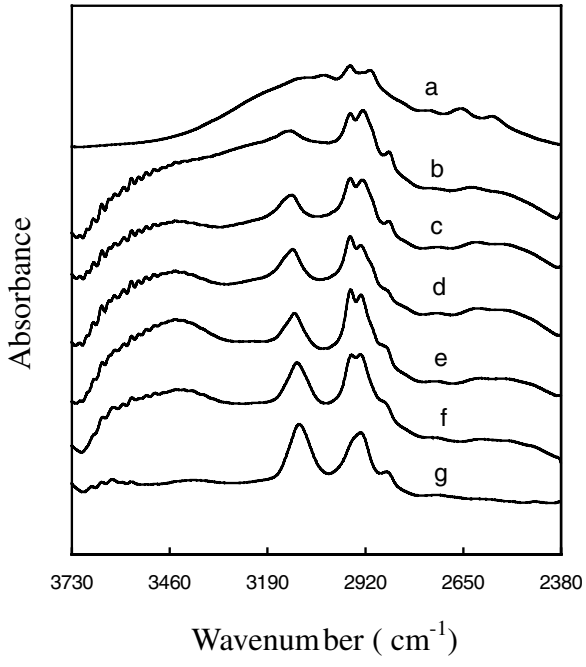

Fig. 5. FT-IR spectra of PSI100/PVI blends: (a) 0; (b) 20; (c) 40; (d) 50; (e) 60; (f) 80 and (g) 100 wt% PVI.

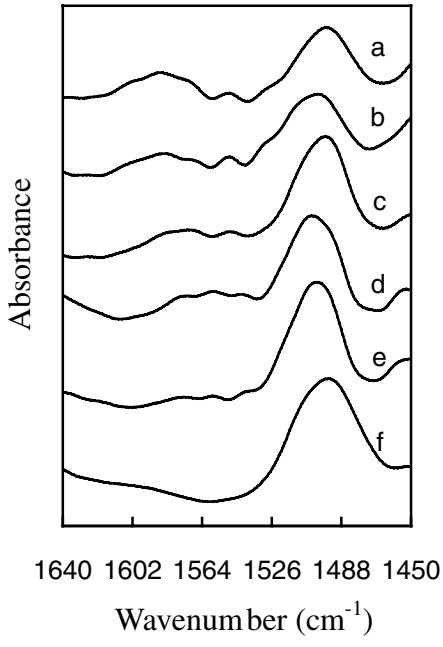

Fig. 7. FT-IR spectra of PSI*X*/PVI (50:50) blends: (a) PSI100; (b) PSI76; (c) PSI60; (d) PSI41; (e) PSI23 and (f) PVI.

Fig. 6 shows the spectra in the carbonyl region and the stretching vibration of C–C and C–N region of PSI100/PVI blends, along with those of the pure components. As shown in the figure, PSI100 exhibits a rather broad carbonyl stretching band around 1713 cm^{-1} comprising two overlapping carbonyl stretching modes of free and self-associated carboxylic acid groups. The latter is at a lower wavenumber than the former. In the PSI100/PVI blends, the carbonyl stretching band narrows sharply with the band center moving to 1728 cm^{-1}. Such a change can be attributed to the ionization of carboxylic acid groups. When ionization occurs, resonance is possible between the two C–O bond in the COO^- group and, consequently, the characteristic carbonyl stretching absorption vanished [25]. The characteristic anti-symmetric vibration band of COO in the 1550–1600 cm^{-1} region is also shown in Figs. 6 and 7, especially in the blends with low carboxypropyl content of sample PSI*X* which is indicated in Fig. 7. Thus it is evident that ionic interactions are present in PSI100/PVI blends.

The assignment of spectral bands to the various vibration modes has been reported for PVI [24,26,27]. Van de Grampel et al. [27] have studied the effect of protonation of PVI on its FT-IR spectrum in the presence of poly(methacrylic acid). They reported that in addition to the stretching vibration of C–C and C–N of PVI at 1500 cm^{-1}, new bands at 1573 and 1544 cm^{-1} appeared upon protonation. As shown in Fig. 6, PVI exhibits a strong ring vibration mode at 1500 cm^{-1}. Upon mixing PVI with PSI100, the development of ring vibration modes at 1582 and 1544 cm^{-1} can be observed. With increasing PSI100 content in the blends, the intensity of the 1500 cm^{-1} band decreases, but the intensities of the bands at 1582 and 1544 cm^{-1} increase gradually, showing that the extent of protonation of imidazole ring in the blends increases with increasing PSI100 content. As mentioned earlier, the characteristic anti-symmetric vibration of COO^- also appears in the 1550–1600 cm^{-1} region. Thus, the 1582 cm^{-1} band is contributed by both the protonated PVI and the ionized PSI100, and it is difficult to make a quantitative studies on the degree of protonation of PVI. Meanwhile, the stretching mode of C=N at 1647 cm^{-1} shifts to 1666 cm^{-1} in the blends.

Fig. 7 shows the FT-IR spectra of various PSI*X*/PVI (50:50) blends between 1640 and 1450 cm^{-1}. As shown in the figure, the intensity of the 1500 cm^{-1} band decreases, but the intensities of the bands at 1582 and 1544 cm^{-1} increase gradually with increasing carboxypropyl content of PSI*X*. At the same time, the anti-symmetric band of COO^- at 1557 cm^{-1} in the PSI23/PVI blends shifts to higher wavenumbers with increasing carboxypropyl content of PSI*X*. Therefore, the results indicate that the intensity of ionic interaction increases with increasing carboxypropyl content of PSI*X*.

In summary, the FT-IR studies show the existence of ionic interaction in the PSI*X*/PVI blends and the intensity of such interactions depends on the carboxypropyl content of PSI*X*.

3.3. XPS Characterization

Recent studies have shown that XPS is useful to study specific interactions in polymer blends and complexes [18,28–34]. Since the BE of a core-level electron depends on its chemical environment within the molecules, the XPS spectrum provides information on the type and number of different species of a given atom in the molecules.

Fig. 8 shows the N1s spectra of PVI and the PSI100/PVI blends. For PVI, the symmetrical N1s peak can be deconvoluted into two component peaks, one at 398.6 eV and the other at 400.6 eV. The peak at 400.6 eV is attributed to the

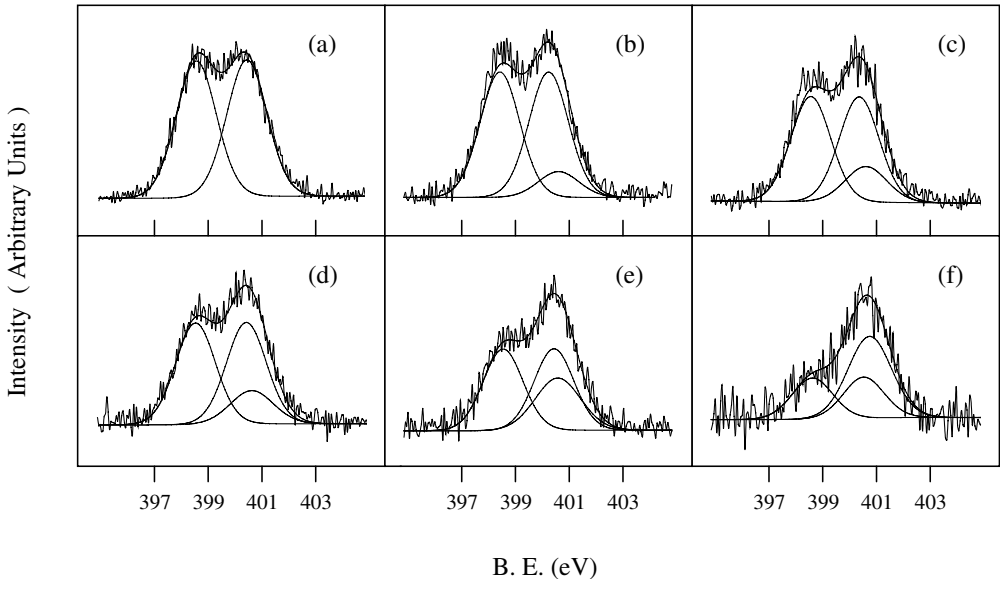

Fig. 8. N1s core-level spectra of PVI/PSI100 blends: (a) 100; (b) 80; (c) 60; (d) 50; (e) 40 and (f) 20 wt% PVI.

Table 2
Characteristics of PSI100/PVI blends

Blend sample number	1	2	3	4	5
Mole fraction of PSI100 in the bulk	0.14	0.30	0.39	0.49	0.72
Mole fraction of PSI100 in the surface region	0.32	0.46	0.54	0.59	0.77
N1s BE (eV) of protonated N(3)	400.8	400.8	400.7	400.7	400.8
Fraction of protonated N(3)	0.19	0.23	0.25	0.34	0.53

nitrogen (denoting as N(1)) through which the imidazole ring is attached to the main chain. The peak at 398.6 eV is attributed to the other nitrogen (denoting as N(3)) in the imidazole ring. This assignment is based on the consideration that the lone pair electrons of N(1) are involved in π-bonding, and thus the electronic environment of N(1) is more electron-deficient than that of N(3), leading to a higher BE of N(1). The N1s peaks of the blends are broader and asymmetric, and each can be resolved into three component peaks, with two of them remaining at the same positions as those in the pure PVI and the third one appearing at 400.8 eV. Our recent studies have shown that when the nitrogen of pyridine, piperidine or imidazole is protonated, the BE value of N1s is increased by 2.0 eV or more. On the other hand, if the nitrogen is involved in hydrogen-bonding interaction, the BE is increased by less than 1.0 eV [18,28–31]. The peak at 400.8 eV is the N(3) in PVI that is protonated by PSI100. Because of the conjugation effect, the electronic environment of N(1) becomes electron-deficient once N(3) is protonated. As a result, the peak at 400.8 eV is composed in equal parts of protonated N(3) and high-BE N(1) arising from the conjugation effect when N(3) is protonated. The result indicates that the intermolecular interaction in PSI100/PVI blends is ionic interaction.

Since the peak at 400.8 eV is due to protonated N(3) and also to N(1) affected by the conjugation effect, the fraction of protonated N(3) atoms can be calculated from one-half of the area of the peak at 400.8 eV. As shown in Table 2, the fraction of the protonated nitrogen atom increases with increasing PSI100 content in the complex. The conclusion agrees with that revealed by FT-IR studies as mentioned earlier.

Fig. 9 shows the N1s core-level spectra of several PSI*X*/PVI (50:50) blends. As shown in the figure, increasing carboxypropyl content of the PSI*X* sample leads to an increase in the intensity of the peak at 400.8 eV, showing that more N(3)s have been protonated when the PSI*X* sample contains more carboxypropyl groups. As a result, the intensity of ionic interaction increases with the increasing carboxypropyl content of the PSI*X* sample.

The surface compositions of the blends can be calculated from the Si/N peak area ratios after correction with the appropriate sensitivity factors. As shown in Table 2, the mole fraction of PSI100 in the surface region of a blend is higher than that in the bulk. The surface region of a polymer blend is enriched with the polymer with a lower surface energy [35–37]. Since polysiloxanes are noted for their lower surface energies, one would expect the surface regions of the PSI100/PVI blends to be enriched with PSI100, and this is confirmed experimentally.

The main difference between the present PSI*X*/PVI system and the previously reported PSI*X*/PVPy system is the nature of intermolecular interactions. The nitrogens of P2VPy and P4VPy are not protonated by PSI*X* and the two dissimilar polymers interact through hydrogen-bonding interactions. In contrast, the nitrogens of PVI are protonated by PSI*X* and the two polymers interact through ionic interactions. The stronger basicity of imidazole apparently facilitates its protonation by PSI*X*. The stronger ionic

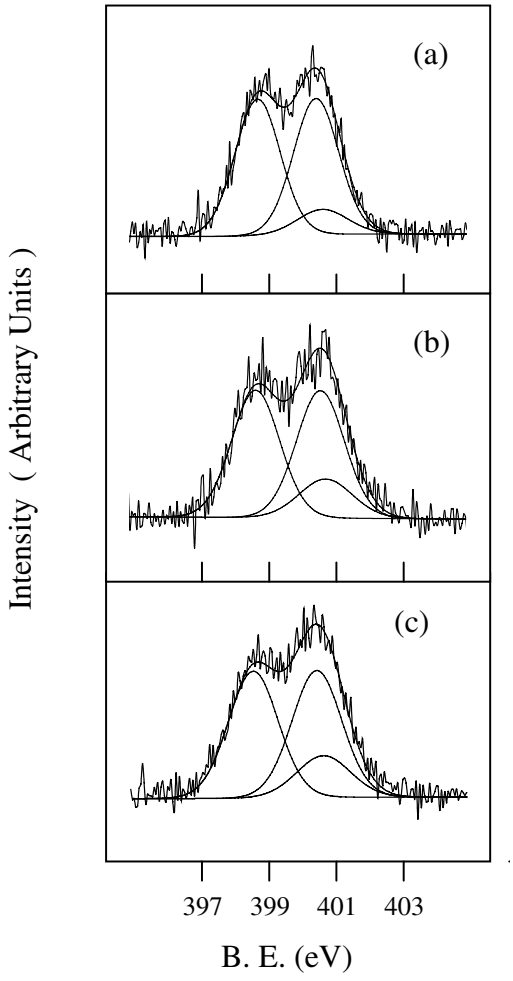

Fig. 9. N1s core-level spectra of PSI*X*/PVI (50:50) blends: (a) PSI23; (b) PSI76 and (c) PSI100.

interactions in the PSI*X*/PVI blends are also reflected by the absence of LCST behavior and the more significant positive deviations in their T_g values. The present study thus demonstrates that the nature of intermolecular interaction depends strongly on the basicity of the proton-accepting polymer.

4. Conclusions

PDMS is immiscible with PVI throughout the entire composition range, but the incorporation of carboxylic acid groups to PDMS leads to an improvement in its miscibility. When 23 mol% of the repeat units of PDMS has been modified, the resulting PSI23 is miscible with PVI throughout the entire composition range. Most of the miscible PSI*X*/PVI blends show positive deviations in their T_g values. None of the miscible blends shows LCST behavior prior to degradation. Both FT-IR and XPS show that PSI*X* interacts with PVI through ionic interactions.

References

[1] Douglas EP, Sakurai K, MacKnight WJ. Macromolecules 1991;24:6776.
[2] Lu S, Pearce EM, Kwei TK. J Polym Sci Part: A Polym Chem 1994;32:2607.
[3] Lu S, Pearce EM, Kwei TK. J Macromol Sci — Pure Appl Chem 1994;A31:1535.
[4] Lu S, Pearce EM, Kwei TK. Polym Adv Technol 1996;7:553.
[5] Lu S, Pearce EM, Kwei TK, Chu EY. J Polym Sci Part A: Polym Chem 1996;34:3163.
[6] Qiu X, Jiang M. Polymer 1994;35:5084.
[7] Qiu X, Jiang M. Polymer 1995;36:3601.
[8] Zhou H, Xiang M, Chen W, Jiang M. Macromol Chem Phys 1997;198:809.
[9] Jiang M, Li M, Xiang M, Zhou H. Adv Polym Sci 1999;146:121.
[10] Bouslah N, Hammachin R, Amrani F. Macromol Chem Phys 1999;200:678.
[11] Parada LG, Cesteros LC, Meaurio E, Katime I. Macromol Chem Phys 1997;198:2505.
[12] Parada LG, Meaurio E, Cesteros LC, Katime I. Macromol Chem Phys 1998;199:1597.
[13] Katime I, Parada LG, Meaurio E, Cesteros LC. Polymer 2000;41:1369.
[14] Santra RN, Roy S, Bhowmick AK, Nando GB. Polym Engng Sci 1993;33:1352.
[15] Chu EY, Pearce EM, Kwei TK, Yeh TF, Okamoto Y. Makromol Chem, Rapid Commun 1991;12:1.
[16] Li X, Goh SH, Lai YH, Wee ATS. Polymer 2000;41:6563.
[17] Luo XF, Goh SH, Lee SY. Macromol Chem Phys 1999;200:399.
[18] Luo XF, Goh SH, Lee SY, Huan CHA. Macromol Chem Phys 1999;200:874.
19 Kwei TK. J Polym Sci, Polym Lett Ed 1984;22:307.
[20] Pennachia JR, Pearce EM, Kwei TK, Bulkin BJ, Chen JP. Macromolecules 1986;19:973.
[21] Velada JL, Cesteros LC, Meaurio E, Katime I. Polymer 1995;36:2765.
[22] Cesteros LC, Velada JL, Katime I. Polymer 1995;36:3183.
[23] Lee JY, Painter PC, Coleman MM. Macromolecules 1988;21:954.
[24] Lippert JL, Robertson JA, Havens JR, Tan JS. Macromolecules 1985;18:63.
25 Bellamy LJ. The infra-red spectra of complex molecules. London: Methuen, 1992.
[26] Eng FP, Ishida H. J Appl Polym Sci 1986;32:5021.
[27] Van de Grampel HT, Tan YY. Challa. Macromolecules 1992;25:1041.
[28] Goh SH, Lee SY, Dai J, Tan KL. Polymer 1996;37:5305.
[29] Zhou X, Goh SH, Lee SY, Tan KL. Appl Surf Sci 1998;126:141.
[30] Luo XF, Goh SH, Lee SY, Tan KL. Macromolecules 1998;31:3251.
[31] Zhou X, Goh SH, Lee SY, Tan KL. Polymer 1998;39:3631.
[32] Zeng XM, Chan CM, Weng LT, Li L. Polymer 2000;41:8321.
[33] Li L, Chan CM, Weng LT. Polymer 1998;39:2335.
[34] Li L, Chan CM, Weng LT, Xiang ML, Jiang M. Macromolecules 1998;31:7248.
[35] Bhatia QS, Pan DH, Kobertein JT. Macromolecules 1988;21:2166.
[36] Schmidt JJ, Gardella JrJA, Salvati JrL. Macromolecules 1989;21:4489.
[37] Goh SH, Chan HSO, Tan KL. Appl Surf Sci 1991;52:1.